Monitoring Land-Surface Snow Conditions from SSM/I Data Using an Artificial Neural Network Classifier

Changyi Sun, Christopher M. U. Neale, Jeffrey J. McDonnell, and Heng-Da Cheng, *Senior Member, IEEE*

***Abstract*—Previously developed Special Sensor Microwave/ Imager (SSM/I) snow classification algorithms have limitations and do not work properly for terrain where forests overlie snow cover. In this study, we applied unsupervised cluster analysis to separate SSM/I brightness temperature (T_B) observations into groups. Six desired snow conditions were identified from the clusters; both sparse- and medium-vegetated region scenes were assessed. Typical SSM/I T_B signatures for each snow condition were determined by calculating the mean T_B value of observations for each channel in the corresponding cluster. A single-hidden-layer artificial neural network (ANN) classifier was designed to learn the SSM/I T_B signatures. An error backpropagation training algorithm was applied to train the ANN. After training, a winner-takes-all method was used to determine the snow condition. Results showed that the ANN classifier was able to outline not only the snow extent but also the geographical distribution of snow conditions. This study confirms the potential of using cluster means in ANN supervised learning, and suggests a nonlinear retrieval method for inferring land-surface snow conditions from SSM/I data over varied terrain.**

I. Introduction

MONITORING land-surface snow conditions throughout the snow season is essential for understanding regional hydrologic response and global climatic feedbacks. The Special Sensor Microwave/Imager (SSM/I) radiometer, onboard the Defense Meteorological Satellite Program (DMSP) satellites, is a useful tool for classifying snow because it is sensitive to the changes in snow physical and dielectric properties. The SSM/I is a seven-channel, four-frequency, linearly polarized, passive microwave radiometric system; it measures both vertically (V) and horizontally (H) polarized brightness temperatures (T_Bs) at 19.35, 37.0, and 85.5 GHz and only vertical polarization at 22.235 GHz [1]. Each day, 14.1 full orbit resolutions are acquired, including ascending (south to north) and descending (north to south) overpasses.

Many SSM/I snow classification algorithms have been developed [2]–[4]. In general, these methods have employed statistical linear relationship of polarization information, in terms of thresholds of certain T_B combinations, between different land surface features to form the classification rules. However, these rules are restricted to land surfaces with uniform snow conditions. Where evergreen forests overlie snowpack, the developed algorithms may misidentify those forested snow covers with snow-free areas. As indicated in [5], vegetation, especially coniferous trees, will mask the microwave emission from the snow below, thereby resulting in a higher T_B that makes the classification rules uncertain.

In complex terrain situations, statistical regression is often unsuitable because there are too many random variables involved in the characterization of microwave response, making the problem extremely nonlinear. According to [6], some of the most complex remote sensing problems can be handled with unsupervised cluster analysis, which separates the observed data vectors into groups. Cluster analysis has the advantage of making no *a priori* assumptions about the possible classes, providing objective indications of the information embedded in multidimensional data sets. The study of [7] shows that typical T_B signatures for a variety of snow classes can be derived from the average (cluster mean) of all T_B data at a given frequency in each class defined by clustering process.

Recently, the use of artificial neural network (ANN) with supervised learning to retrieve snow properties from passive microwave data has been addressed [8]–[10]. Studies have shown that ANN's have the potential to learn T_B patterns, where previously the complexity and nonlinearity in the variables made them difficult to define using empirical regression approaches.

In neural computing, error backpropagation training [11] is the most widely used learning method in the development of an ANN classifier. This method requires that the input and the desired output must be provided during training; consequently, the selection of input/output data pairs is essential to the success in ANN generalization. Following [12], an ANN trained from only cluster means showed a reliable generalization capability in pattern classification.

In this study, we propose a new framework where typical SSM/I T_B signatures of desired snow conditions are interpreted from unsupervised cluster analysis, and then used as a prelude to supervised learning in an ANN classifier. In this way, the ANN learns only the central tendency of the clusters, in terms of geophysical significance of the snow conditions, instead of all random information from the data. We explore

Manuscript received September 5, 1995; revised February 14, 1996. This work was supported by the NASA WetNet Project under Contract NAG8-897 and by the Utah Agricultural Experiment Station.

C. Sun, C. M. U. Neale, and H.-D. Cheng are with Utah State University, Logan, UT 84322-5215 USA (e-mails: csun@indigo.ecob.usu.edu; cneale@cc.usu.edu; cheng@hengda.cs.usu.edu).

J. J. McDonnell is with the State University of New York College of Environmental Science and Forestry, Syracuse, NY 13210 USA.

Publisher Item Identifier S 0196-2892(97)04470-7.

the above concept operationally for inferring land-surface snow conditions from SSM/I data over varied terrain.

II. Study Site and Data Integration

The study area is bounded by latitude of 40°N to 45°N and longitude of 100°W to 115°W, including both plains and mountainous regions of the western United States. This area contains a variety of sparse- and medium-vegetated terrain. Data of SSM/I T_B, normalized difference vegetation index (NDVI), and ground-based snow measurements from October 1, 1989 to May 30, 1990 in the area were used.

The SSM/I T_B observations from the DMSP-F8 satellite were obtained from the Naval Research Laboratory. Due to the degradation of the 85.5 GHz channels on DMSP-F8 satellite after March 1988, only T_B data from the five lower frequency channels, denoted as T19V, T19H, T22V, T37V, and T37H, were employed.

The NDVI was calculated from the visible and near-infrared digital values of the NOAA Advanced Very High Resolution Radiometer (AVHRR). NDVI is useful for characterizing the vegetation density over large regions [13]. These data have a valid greenness value range from 110 to 160 [14]. A monthly maximum scaled NDVI data set [15] was obtained for the reference ground truth vegetation.

Ground-based measurements of daily snow water equivalent (SWE), and maximum, minimum and average air temperature over mountainous terrain were obtained from the Soil Conservation Service (SCS) SNOTEL (SNOwpack TELemetry) system [16]. Daily snow depth (SD), maximum and minimum air temperature, and air temperature at the measuring time in the plains were derived from the NOAA cooperative weather observing network [17]. These ground-based data were used to estimate snow conditions at weather stations.

Land-surface snow condition of each SNOTEL or NOAA weather station at the DMSP-F8 local crossing time (either 0600 or 1800) was classified as: 1) snow-free if SWE or SD was equal to zero; 2) dry snow if SWE or SD increased from the previous date and the concurrent air temperature was less than or equal to 0 °C, 3) wet snow if SWE or SD was not equal to zero and the concurrent air temperature was greater than 0 °C; or 4) refrozen snow if the concurrent air temperature was below freezing and the snow condition of the previous date was either wet or refrozen. Because of the lack of SWE data, SD data at NOAA stations were converted to SWE by assuming a snow density of 0.2 for dry, 0.3 for wet, and 0.4 for refrozen snow.

For the SNOTEL stations, air temperatures at 0600 and 1800 (the SSM/I overpass time) were defined as the daily minimum and average air temperature, respectively. For NOAA weather stations, air temperatures derived between 0400 and 0700 and between 1600 and 1900 intervals were used for the 0600 and 1800 SSM/I overpass data. If air temperatures were not recorded between these intervals, the air temperature at 0600 was equal to the minimum air temperature and that at 1800 was extrapolated as follows: the maximum air temperature was assumed at 1400 and was linearly decreased to the temperature at observing time if after 1400, or the maximum air temperature of the previous day was decreased to the temperature at observing time if before 1400.

Since the latitude/longitude coordinates of the SSM/I footprints change with each overpass, a neighborhood merging method was employed to link the multisource data into a single database. This was done by searching the AVHRR pixels and ground weather stations within a 15-km radius of the SSM/I latitude/longitude location (i.e., approximately the size of a 37.0 GHz footprint). Average NDVI, average SWE, and dominant snow condition were determined for the corresponding footprint.

Only data of SSM/I footprints with snow-covered land surface (average SWE >0 mm) were considered as valid elements in the database. In addition, based on the land-surface-type classification rules in [2], each SSM/I footprint was checked for flooding condition (T22V–T19V >4 K) and precipitating condition (T19V >268 K). Data of these conditions, if existed, were discarded from the database.

III. Cluster Analysis of SSM/I T_B Data

Two clustering methods, the average linkage and centroid method [18], were used to explore the possible clusters in the database with respect to five SSM/I T_B variables of lower frequency channels. Clusters suggested by the cubic clustering criterion (CCC) [19] were examined from the smallest number of clusters to higher ones until the desired snow conditions [i.e., dry snow with sparse (DsSv) or medium (DsMv) vegetation density, wet snow with sparse (WsSv) or medium (WsMv) vegetation density, and refrozen snow with sparse (RsSv) or medium (RsMv) vegetation density] were all defined. In each number of clusters, the cluster means, in terms of five mean T_B values (typical T_B signature) and mean NDVI, were determined for each cluster. A hypothetical true snow condition, if detected, was then assigned to the cluster according to its cluster means in relation to the emission behavior of snow cover and vegetation density. Ultimately, only data from the six most distinguishable clusters for the desired snow conditions were selected.

Table I shows the cluster means of six land-surface snow conditions defined by the two clustering methods at different suggested number of clusters. Generally, refrozen snow and sparse-vegetated dry snow conditions were more easily distinguished in a smaller number of clusters than wet snow and medium-vegetated dry snow conditions. The mean NDVI values of the selected clusters were all below 110 (Table I) suggesting a nonvegetated area according to [14]. Such low values could be due to the heterogeneous vegetation density in the study area and the integration of NDVI from AVHRR high spatial resolution (1 km) to SSM/I low resolution (30 km at 37 GHz). Nevertheless, higher values were associated with the medium-vegetated snow cover for dry, wet, and refrozen conditions, suggesting the NDVI is usable for characterizing microwave responses of different vegetated snow conditions.

Fig. 1 shows the typical SSM/I T_B signatures defined for the six snow conditions, using average linkage and centroid method. Both methods provided similar T_B patterns of snow conditions. Mean T_B values of medium-vegetated snow were

TABLE I
CLUSTER MEANS OF LAND-SURFACE SNOW CONDITIONS

Clustering Method	Snow Condition	Cluster Means T37V	T37H	T22V	T19V	T19H	NDVI	# of Clusters by CCC
Average Linkage	DsSv	245.97	234.64	252.95	255.21	241.98	90	29
	DsMv	252.03	245.90	258.53	260.57	252.76	105	35
	WsSv	259.77	250.71	261.44	261.39	247.39	103	43
	WsMv	259.23	253.74	263.12	264.71	257.40	108	43
	RsSv	208.68	200.04	237.61	244.39	228.43	52	9
	RsMv	231.97	225.92	248.25	252.32	243.27	93	43
Centroid Method	DsSv	245.27	234.53	252.43	254.75	242.03	91	39
	DsMv	250.85	244.37	257.61	259.73	251.48	102	49
	WsSv	259.31	250.40	260.45	259.61	243.91	107	43
	WsMv	260.07	254.24	264.12	265.62	257.87	109	43
	RsSv	208.68	200.04	237.61	244.39	228.43	52	12
	RsMv	230.63	223.76	247.70	252.01	241.97	87	43

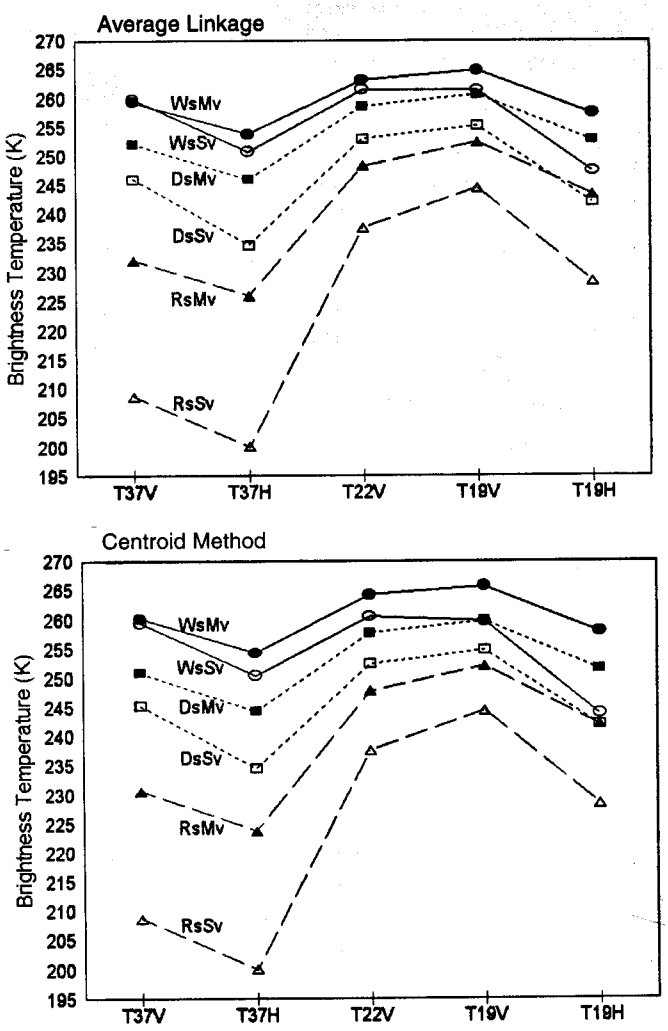

Fig. 1. Typical SSSM/I T_B signatures of six land-surface snow conditions defined by clustering analysis.

higher than those of sparse-vegetated since the overlying vegetation tends to increase the T_B [5], especially at higher frequencies [20]. The refrozen snow conditions were most distinguishable from the others at 37 GHz. This is because the melting and freezing process produces larger snow crystals, which scatter the emission at shorter wavelengths [21]. Mean T_B values of wet snow were the highest for all conditions, since the liquid water at the surface of snowpack can absorb and re-emit the microwave radiation from the snow below [22]. This emission behavior together with the effect of overlying vegetation made microwave signatures of WsSv, WsMv, and DsMv similar, causing the information of these snow conditions to be not apparent when the number of clusters was small (Table I).

In comparison, disagreement was found between ground-based and clustering-based snow conditions (Table II). This could be due to the noise in ground-based estimation. The ground-based snow conditions were interpreted by the estimation of concurrent air temperature of point measurements within each SSM/I footprint. Error could be introduced due to the temporal variability of air temperature, causing different snow conditions to be related to SSM/I footprints of similar T_B patterns. With respect to dry, wet, and refrozen snow, a t-test for testing the null hypothesis that the means of two groups are equal [18] was performed to compare the equality of variances between ground-based data, clustering-based data, and intersection of the two (i.e., data classified consistently by ground-based and clustering methods). Results of probability (p) values (Table III) showed that ground-based and average-linkage-based snow conditions were significantly different at 0.05 level. However, significant agreement (p value >0.05) was found between the intersection and clustering-based data sets. Similar results were also found in data using centroid method.

Accordingly, the above interpretation and justification provide the theoretical and statistical basis for the use of clustering-based SSM/I T_B signatures in ANN supervised training.

IV. ANN TRAINING, VALIDATION, AND TEST DATA

The training data set was created by the input/output pairs of typical T_B signature and corresponding snow condition from each of the six selected clusters. A validation data set, used to evaluate the learning performance of ANN during training, was also prepared. Based on the number of data elements in each selected cluster, the validation data set was formed by including either all data in the cluster if the number of elements was 100 or less, or the upper and lower quartiles

TABLE II
COMPARISON BETWEEN GROUND-BASED AND CLUSTERING-BASED SNOW CONDITIONS

Clustering Method	Clustering-Based Condition and Data Elements		Ground-Based Condition and Data Elements		
			Dry	Wet	Refrozen
Average Linkage	DsSv	237	(112)	12	113
	DsMv	1608	(1005)	72	531
	WsSv	93	37	(26)	30
	WsMv	1123	592	(150)	381
	RsSv	19	9	3	(7)
	RsMv	213	156	5	(52)
Centroid Method	DsMv	216	(111)	11	94
	DsMv	1112	(710)	40	362
	WsSv	24	9	(8)	7
	WsMv	741	336	(121)	284
	RsSv	19	9	3	(7)
	RsMv	167	123	5	(39)

Number in () represents the elements in the intersection of ground-based and clustering-based data sets.

TABLE III
PROBABILITY VALUES OF GROUP MEANS COMPARISONS BETWEEN GROUND-BASED CLASSIFICATION AND INTERSECTION OF THE TWO METHODS

Variable	Ground vs. Clustering			Ground vs. Intersection			Intersection vs. Clustering		
	Dry	Wet	Refrozen	Dry	Wet	Refrozen	Dry	Wet	Refrozen
T37V	0.000	0.000	0.000	0.002	0.000	0.000	0.701	0.001	0.559
T37H	0.000	0.000	0.000	0.000	0.000	0.000	0.042	0.646	0.578
T22V	0.000	0.000	0.000	0.000	0.000	0.000	0.403	0.007	0.881
T19V	0.000	0.000	0.000	0.000	0.000	0.000	0.464	0.108	0.926
T19H	0.000	0.000	0.000	0.000	0.001	0.000	0.005	0.000	0.668

[23] of the data if the number of elements was large. The purpose was to eliminate the possible outliers to ensure that the ANN evaluation was based on data related to the central tendency of the cluster.

The corresponding snow conditions in each training and validation data set were coded as (0.8, −0.8, −0.8, −0.8, −0.8, −0.8) for DsSv, (−0.8, 0.8, −0.8, −0.8, −0.8, −0.8) for DsMv, (−0.8, −0.8, 0.8, −0.8, −0.8, −0.8) for WsSv, (−0.8, −0.8, −0.8, 0.8, −0.8, −0.8) for WsMv, (−0.8, −0.8, −0.8, −0.8, 0.8, −0.8) for RsSv, and (−0.8, −0.8, −0.8, −0.8, −0.8, 0.8) for RsMv to represent the desired outputs in the ANN learning.

Ideally, a test data set is used to measure the generalization capability of a trained ANN in real use; therefore it should be completely independent of the data used in training and validation. Based on the information of NOAA daily weather maps and the availability of SSM/I data, T_B observations from DMSP-F11 satellite over the United States on Jan. 9, 1993 were selected as the test data set. The SSM/I data were provided by the EOS Distributed Active Archive Center (DAAC) at the Marshall Space Flight Center, Global Hydrology and Climate Center, Huntsville, AL.

V. ANN TOPOLOGY AND LEARNING APPROACH

A single-hidden-layer backpropagation ANN, as illustrated in Fig. 2, was implemented. It consisted of one input layer of five nodes representing the inputs T_B of values of lower SSM/I channels, one hidden layer of preferred number of nodes, and one output layer of six nodes for the land-surface snow conditions. Given the number of nodes in each layer from input to output as a sequence, the ANN topology was represented as 5-N-6, where N is the number of hidden nodes. Four ANN topologies, 5-5-6, 5-10-6, 5-20-6, and 5-30-6, were designed for the study. A bias node, functioning similar to a constant in a regression, was connected to the nodes in the hidden and output layers. In addition, nodes of adjacent layers were fully connected with different weights that were initialized at small random values between −0.1 and 0.1.

The error backpropagation training algorithm [24], as described in [11], was applied to train each ANN. This method allows inputs to flow forward through the hidden layer to the output layer and calculates the node outputs (Xi in Fig. 2) in each layer. Inputs are scaled between −1 and 1 for the node outputs in the input layer. However, each node in the hidden layer and output layer decides its output by calculating the net, which is the sum of all its incoming weights multiplied by the node outputs of the previous layer. Then the net is transferred by a hyperbolic tangent (tanh) nonlinear function to give an output between −1 and 1. Mapping error (Ei in Fig. 2) of each node in the output layer is measured by the least squared error between node output (Xi in Fig. 2) and its desired output (Di in Fig. 2). Errors are then propagated backward from the output layer to the input layer to adjust the weights using the delta learning rule [24] to minimize the error, so that the calculated outputs in the output layer are more like the desired outputs.

VI. DEVELOPMENT OF THE ANN CLASSIFIER

Training was conducted by repeating a training cycle for each of the four ANN topologies. The training cycle involved forward feeding T_B values in the training set from input layer

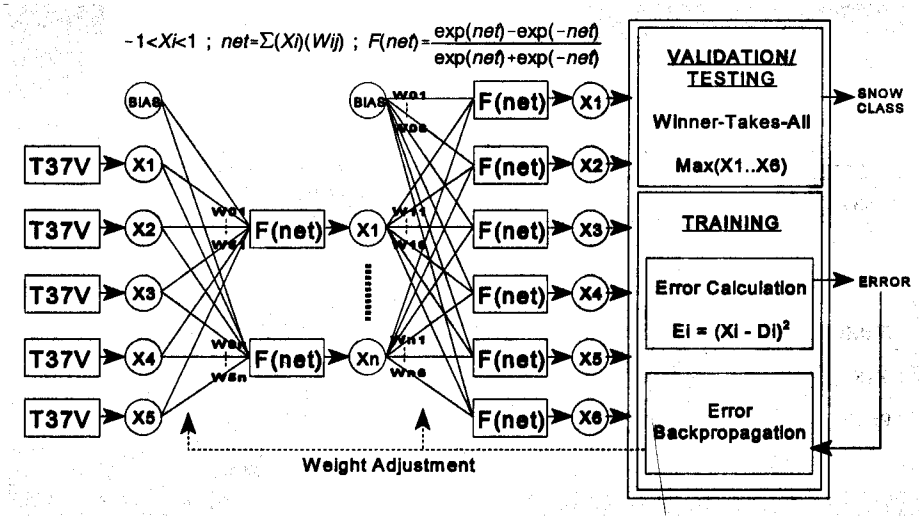

Fig. 2. The design of an artificial neural network classifier.

TABLE IV
LEARNING PERFORMANCE OF THE ANN'S

Clustering Method	ANN Topology	RMS Tolerance	Training Cycles	Error Rate (%)
Average Linkage	5-5-6	0.215	1743	10.9
		0.200	2908	3.9
		0.185	7772	4.6
	5-10-6	0.300	1159	3.4
		0.200	5243	2.4
		0.190	4329	6.6
	5-20-6	0.230	1708	8.7
		0.215	2597	5.6
		0.200	2603	6.0
	5-30-6	0.240	1998	10.1
		0.230	2552	7.2
		0.220	2098	16.9
Centroid Method	5-5-6	0.225	1984	5.5
		0.200	1989	4.9
		0.170	3271	5.5
	5-10-6	0.250	1440	6.7
		0.200	2268	5.5
		0.190	2247	6.1
	5-20-6	0.170	2920	9.8
		0.165	2269	8.0
		0.155	13224	14.7
	5-30-6	0.195	2785	7.4
		0.180	2191	6.1
		0.160	4440	6.7

to output layer to calculate the mapping errors, backward propagating the mapping errors from output layer to input layer to adjust the weights in ANN, and calculating the root-mean-squared (RMS) error after all the input/output pairs in the training set were processed. Training stopped when the RMS error converged to a specified RMS tolerance that was set by trial and error in this study.

The validation data set was used to evaluate the learning performance of each trained ANN. T_B values were forwarded through the ANN and the node outputs in the output layer were calculated. The winner-takes-all method [25] (i.e., the node in the output layer with the highest node output designates the condition) was applied to determine the snow condition for each input of T_B values. Error rate, the percentage of misclassified conditions in the entire validation set, was also determined. An ANN with the minimum error rate was eligible for the SSM/I ANN snow classifier.

Table IV summarizes the training and validation results of the ANN's. The best ANN performance was achieved by the 5-10-6 ANN trained with typical T_B signatures by average

TABLE V
TWO-WAY TABLE OF THE DISTRIBUTION OF SNOW CONDITIONS BY THE ANN CLASSIFIER ON THE INTERSECTION SET OF BOTH AVERAGE-LINKAGE AND GROUND-BASED METHODS

Intersection Data Set	Classification by the ANN Classifier						Total
	DsSv	DsMv	WsSv	WsMv	RsSv	RsMv	
DsSv	72	26	11	3	0	0	112
DsMv	72	572	123	237	0	1	1005
WsSv	0	0	26	0	0	0	26
WsMv	11	14	57	68	0	0	150
RsSv	0	0	0	0	7	0	7
RsMv	4	8	0	0	6	34	52
Total	159	620	217	308	13	35	1352

linkage method and converged at RMS tolerance of 0.2. There is no evidence to conclude that a smaller RMS tolerance may ensure a better ANN performance. The increase in error rate as RMS tolerance decreased could be a sign of overtraining, by which the ANN becomes too specific to the training data rather than learning the general patterns for a successful generalization in validation [26]. In addition, it seems that the number of hidden nodes was not a critical factor in ANN training. The ANN classifier resulted from a number of training processes with different topologies by trial and error.

The two-way frequency table (Table V) outlines the performance of the ANN classifier on the intersection data set in relation to average linkage method (see Table II). Based on the Cochran-Mantel-Haenszel (CMH) statistics that test the null hypothesis of no association [18], significant association (p value <0.05) was found between the row variable and the column variable. This may imply that the ANN learned the central tendency of the clusters defined for each snow condition. However, according to the frequency distribution of the column variables in Table V, most misclassified conditions were related to wet snow, in which certain amount of data elements of DsMv in the intersection set were classified as WsSv or WsMv by the ANN. Although the overlying vegetation and snow wetness could result in similar SSM/I T_B patterns, the clustering method itself could be another factor for the misclassification since there was no guarantee that all of the T_B patterns in a particular cluster were of the same condition. Thus, the use of cluster means in ANN training may benefit from not misleading the ANN with uncertain samples. This allowed the ANN to judge similarity among uncertain data by itself.

VII. APPLICATION OF THE ANN CLASSIFIER

Since the ANN classifier was trained only from the six defined snow conditions, it is not applicable to other surface types. Accordingly, the existing classification rules for flooding and precipitation (see Fig. 3, Rules A) from [2], and the rules for ocean and snowfree (see Fig. 3, Rules B) from [27] were used to filter out those snowfree conditions in test data set before the use of the ANN classifier.

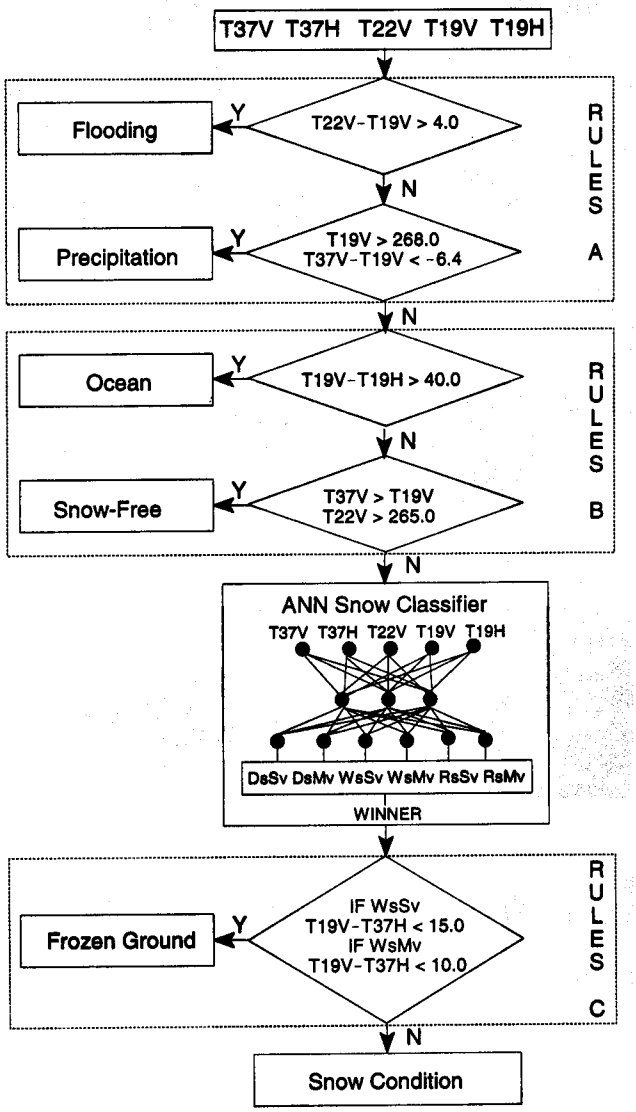

Fig. 3. Flowchart of the application of the ANN classifier.

As indicated in [28], the SSM/I T_B signatures of heavy vegetation, frozen ground and wet snow are similar. It was expected that frozen ground conditions could be embedded in wet snow conditions classified by the ANN. According to the

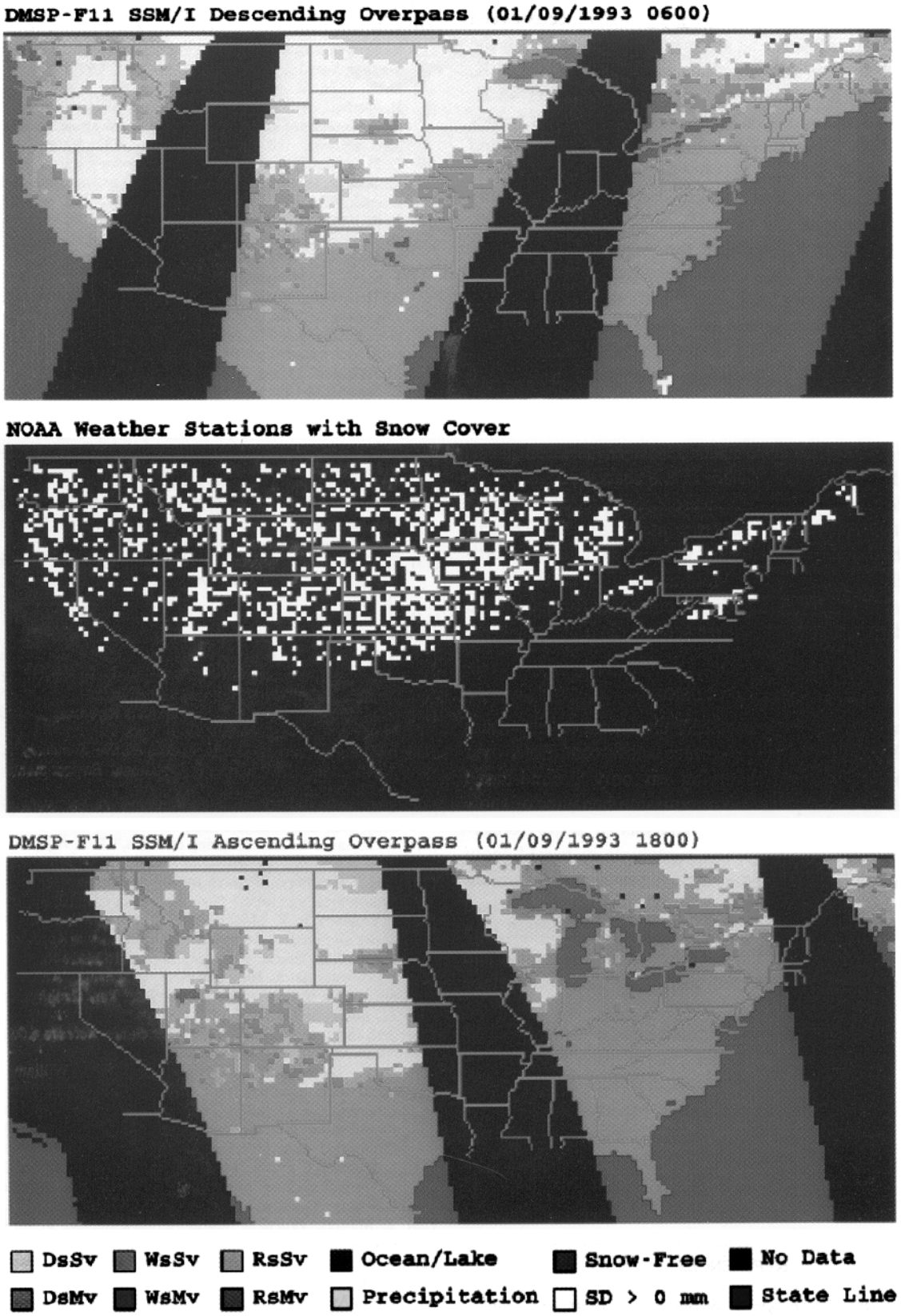

Fig. 4. Case images of snow mapping by the ANN classifier compared with the ground-based snow distribution.

time series interpretation of SSM/I T_B observations at a flat and sparse vegetated footprint in [29], T_B difference between T19V and T37H is sensitive to snow conditions, in which the range of the difference for wet snow is from 10 K to 30 K, dry snow from 30 K to 45 K, and refrozen snow over 45 K. Thus, values of 15 K and 10 K were used as the cutoff values (see Fig. 3, Rules C) to separate the possible frozen ground conditions from WsSv and WsMv, respectively. The latter cutoff value was to take into account the effect of overlying vegetation that could decrease the T_B difference.

Fig. 4 shows the case images of the resulting land-surface snow conditions by the ANN and the snow distribution according to data from NOAA weather stations. Basically, the ANN-based snow extent agreed with the ground-based snow distribution. It is also evident that the ANN-based method was able to outline the geographical snow patterns; i.e., the higher the latitude, more dry snow, and the lower the latitude, more wet snow. Moreover, the DsMv conditions were seen mostly in western mountainous and eastern forested areas, whereas the DsSv conditions were in the central plains. Some of the refrozen snow conditions were accompanied with wet snow, indicating the ongoing presence of melting and freezing processes. The refrozen snow found at the high plains of North Dakota and the areas of Rocky Mountains might be due to the large ice crystals, particularly the depth-hoar, formed in the snowpacks during the early winter season [21].

VIII. Conclusion

To date, no single existing SSM/I classification algorithm has been able to identify land-surface snow conditions over varied terrain. Rather than relying on only ground-based measurements, the interpretation of emission behavior of snow in relation to unsupervised cluster analysis of SSM/I observations provided the prototype T_B signatures of varied snow conditions. Instead of finding the discriminant functions among the clusters, training an ANN with the cluster means showed the potential for pattern recognition. This study resulted in a nonlinear retrieval method that overcomes the drawbacks and limitations of the regression methods for SSM/I land-surface snow classification.

Application of the ANN classifier trained with only snow conditions requires the use of other classification rules to distinguish snowfree surface types. Ultimately, an ANN trained from all possible land-surface types is expected. Further research should focus on the identification of more land-surface types in terms of T_B signatures, especially the heavy vegetation and frozen ground, to improve the efficiency and robustness of the ANN classifier.

References

[1] J. P. Hollinger, *DMSP Special Sensor Microwave/Imager Calibration/Validation, Final Report, Volume I.* Washington, DC: Naval Research Laboratory, 1989.

[2] C. M. U. Neale, M. J. McFarland, and K. Chang, "Land-surface-type classification using microwave brightness temperatures from the Special Sensor Microwave/Imager," *IEEE Trans. Geosci. Remote Sensing*, vol. 28, pp. 829–838, Sept. 1990.

[3] M. J. McFarland and C. M. U. Neale, "Land parameter algorithms validation and calibration," in *DMSP Special Sensor Microwave/Imger Calibration/Validation, Final Report, Volume II*, J. P. Hollinger, Ed. Washington, DC: Naval Research Laboratory, 1991, sec. 9, pp. 1–108.

[4] J. V. Fiore, Jr. and N. C. Grody, "Classification of snow cover and precipitation using SSM/I measurements: case studies," *Int. J. Remote Sensing*, vol. 13, no. 17, pp. 3349–3361, 1992.

[5] D. K. Hall, M. Sturm, C. S. Benson, A. T. C. Chang, J. L. Foster, H. Garbeil, and E. Chacho, "Passive microwave remote and in-situ measurements of arctic and subarctic snow cover in Alaska," in *Remote Sens. Environ.*, vol. 38, no. 3, pp. 161–172, 1991.

[6] D. H. Staelin, "Progress in passive microwave remote sensing: Nonlinear retrieval techniques," in *Remote Sensing of Atmospheres and Oceans*, A. Deepak, Ed. San Diego, CA: Academic, 1980, pp. 259–274.

[7] S. R. Rotman, A. D. Fisher, and D. H. Staelin, "Analysis of multiple-angle microwave observations of snow and ice using cluster-analysis techniques," *J. Glaciology*, vol. 27, no. 95, pp. 89–97, 1981.

[8] J. Key, J. A. Maslanik, and A. J. Schweiger, "Classification of merged AVHRR and SMMR arctic data with neural networks," *Photogramm. Eng. Remote Sens.*, vol. 55, no. 9, pp. 1331–1338, 1989.

[9] A. T. C. Chang and L. Tsang, "A neural network approach to inversion of snow water equivalent from passive microwave measurements," *Nordic Hydrol.*, vol. 23, no. 3, pp. 173–182, 1992.

[10] C. Sun, H. D. Cheng, J. J. McDonnell, and C. M. U. Neale, "Identification of mountain snow cover using SSM/I and artificial neural network," in *Proc. 1995 Int. Conf. Acoustics, Speech, Signal Processing*, 1995, pp. 3451–3454.

[11] J. M. Zurada, *Introduction to Artificial Neural Systems.* St. Paul, MN: West, 1992, ch. 4, pp. 163–250.

[12] C. Sun and H. D. Cheng, "The use of class means in error backpropagation training for species identification of iris data," in *Proc. Joint Conf. Information Sciences*, 1995, pp. 556–559.

[13] G. G. Gutman, "Vegetation indices form AVHRR: an update and future prospects," *Remote Sens. Environ.*, vol. 35, nos. 2 & 3, pp. 121–136, 1991.

[14] K. B. Kidwell, *Global Vegetation Index User's Guide.* Washington, DC: NOAA Natioanl Geophysical Data Center, 1994.

[15] A. M. Hittelman, L. W. Row, J. J. Kineman, R. E. Habrmann, and D. A. Hastings, *Global View CD-ROM's and User's Manual (1994 Edition).* Boulder, CO: NOAA National Geophysical Data Center, 1994.

[16] SCS, *Snow Survey and Water Products Reference.* Portland, OR: SCS West National Technical Center, 1988.

[17] NOAA, *Surface Land Daily Cooperative Summary of the Day TD-3200.* Asheville, NC: NOAA National Environmental Satellite Data and Information Service, 1989.

[18] SAS Institute Inc., *SAS/STAT User's Guide, Release 6.03 Edition.* Cary, NC: SAS Institute Inc., 1988.

[19] W. S. Sarle, "Cubic clustering criterion," *Tech. Rep. A-108.* Cary, NC: SAS Inc., 1983.

[20] B. J. Choudhury, "Passive microwave remote sensing contribution to hydrological variables," *Surv. Geophys.*, vol. 12, pp. 63–84, 1991.

[21] F. T. Ulaby, R. K. Moore, and A. K. Fung, *Microwave Remote Sensing: Active and Passive, Volume III: From Theory to Applications.* Dedham, MA: Artech House, 1986, ch. 19, pp. 1522–1646.

[22] J. L. Foster, D. K. Hall, and A. T. C. Chang, "An overview of passive microwave snow research and results," *Rev. Geophys. Space Phys.*, vol. 22, no. 2, pp. 195–208, 1984.

[23] SAS Institute Inc., *SAS Procedures Guide, Release 6.03 Edition.* Cary, NC: SAS Institute Inc., 1988.

[24] D. E. Rumelhart, G. E. Hinton, and R. J. Williams, "Learning internal representations by error propagation," in *Parallel Distributed Processing: Explorations in the Microstructure of Cognition, Volume 1, Foundations*, J. A. Feldman, P. J. Hayes, and D. E. Rumelhart, Eds. Cambridge, MA: MIT Press, 1986. ch. 8, pp. 318–362.

[25] L. Prechelt, "PROBEN I—A set of neural network benchmark problems and benchmarking rules," Tech. Rep. 21/94, Karlsruhe University, Karlsruhe, Germany, 1994.

[26] T. Masters, *Practical Neural Network Recipes in C++.* San Diego, CA: Academic, 1993, ch. 10, pp. 173–186.

[27] N. C. Grody and A. Basist, "SSM/I snow cover maps of the U.S.," NOAA National Operational Hydrologic Remote Sensing Center, 1995. Available from anonymous FTP: ftp.nohrsc.nws.gov Directory: pub/bbs/ssmi File: ssmi.txt.

[28] J. Hollinger, R. Lo, G. Poe, R. Savage, and J. Peirce, *Spacial Sensor Microwave/Imager User's Guide.* Washington, DC: Naval Research Laboratory, 1987, ch. 4, pp. 66–112.

[29] C. Sun, C. M. U. Neale, and J. J. McDonnell, "The relationship between snow wetness and air temperature and its use in the development of an SSM/I snow wetness algorithm," in *Proc. AGU 15th Annu. Hydrology Days*, 1995, pp. 271–280.

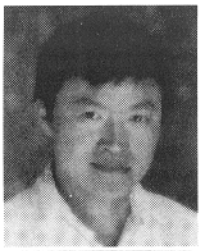

Changyi Sun was born in Taipei, Taiwan, R.O.C. He received the B.S. degree in 1988 from Colorado State University, Fort Collins, and the M.S. degree in 1992 and the Ph.D. degree in 1996 from Utah State University (USU), Logan, all in watershed science.

He was a Research Assistant, Department of Biological and Irrigation Engineering, USU, from 1991 to 1996, involved with the development and improvement of algorithms for snow and soil moisture parameter retrievals using the Special Sensor Microwave/Imager (SSM/I). His research interests are in the areas of global moisture studies from remote sensing.

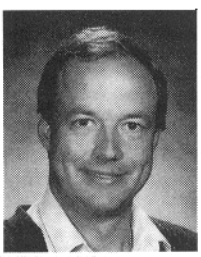

Christopher M. U. Neale received the civil engineering degree from the Escola de Engenharia Maua, Sao Caetano do Sul, Brazil, in 1980, and the M.S. and Ph.D. degrees were in agricultural engineering from Colorado State University, Fort Collins, in 1983 and 1987, respectively.

He is currently an Associate Professor, Department of Biological and Irrigation Engineering, Utah State University (USU), Logan. He has over 15 years of experience in applied remote sensing in the shortwave and longwave part of the electromagnetic spectrum. He was a member of the SSM/I calibration/validation team tasked with developing and validating retrieval algorithms for the first SSM/I instrument (F8), launched in 1987. He has since been conducting research in the retrieval of surface moisture, land surface temperature and snow parameters with the SSM/I. He developed the USU airborne multispectral video/radiometer system which flies on a dedicated remote sensing aircraft. Multispectral imagery from this system has been used in numerous applications in natural resource and agricultural monitoring and mapping.

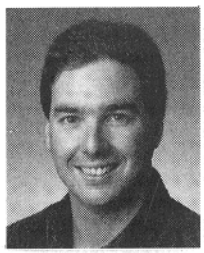

Jeffrey J. McDonnell received the Ph.D. degree from the University of Canterbury, U.K., the M.Sc. degree from Trent University, Peterborough, Ont., Canada, and the B.Sc. degree from the University of Toronto, Toronto, Ont.

He is Associate Professor of Water Resources, State University of New York College of Environmental Science and Forestry, Syracuse. His research focuses on subsurface flow processes through the use of naturally-occurring stable isotopes, water chemistry and soil physics techniques.

Dr. McDonnell has received awards for his research from the Canadian Society of Petroleum Geologists, New Zealand Geological Society, Association of American Geographers and in 1987 was presented the Horton Research Grant from the American Geophysical Union. He serves on several committees of AGU, IAHS and UNESCO. He is Associate Editor for *Water Resources Research* and on the Editorial Board for *Hydrological Processes*.

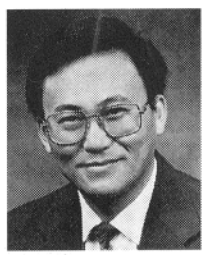

Heng-Da Cheng (S'81–M'85–SM'90) received the Ph.D. degree in electrical engineering from Purdue University, West Lafayette, IN, in 1985.

He is an Associate Professor, Department of Computer Science, and an Adjunct Associate Professor, Department of Electrical and Computer Engineering, Utah State University, Logan. His research interests include parallel processing, parallel algorithms, artificial intelligence, image processing, pattern recognition, computer vision, fuzzy logic, genetic algorithms, neural networks, and VLSI architectures. He has published more than 140 technical papers and is the co-editor of the book, *Pattern Recognition: Algorithms, Architectures and Applications* (Singapore: World Scientific, 1991).

Dr. Cheng has been listed in *Who's Who in the World, Who's Who in Science and Engineering, Who's Who in America, Men of Achievement, 2000 Notable American Men*, etc. He is a member of the Association of Computing Machinery. He is an Associate Editor of *Pattern Recognition* and an Associate Editor of *Information Sciences*. He was Program Co-Chairman of Vision Interface'90, Program Committee Member of Vision Interface'92 and of Vision Interface'96, Session Chair and Member of Best Paper Award Evaluation Committee of International Joint Conference on Information Sciences (1994 and 1995), Program Committee Member of the 1995 International Conference on Tools with Artificial Intelligence, and Program Committee Member of the 17th International Conference on Computer Processing of Oriented Languages, 1997.